A General Synthesis Approach toward Halloysite-Based Composite Nanotube

Cuiping Li, Jiguang Liu, Xiaozhong Qu, Zhenzhong Yang

State Key Laboratory of Polymer Physics and Chemistry, Institute of Chemistry, Chinese Academy of Sciences, Beijing 100190, China

Received 30 July 2008; accepted 4 November 2008
DOI 10.1002/app.29652
Published online 23 February 2009 in Wiley InterScience (www.interscience.wiley.com).

ABSTRACT: We have demonstrated a general template synthesis halloysite-based composite nanotube. Starting from a parent halloysite nanotube, polymer composite nanotubes were synthesized by atom transfer radical polymerization (ATRP). The shell thickness and the cavity size of the polymer composite nanotubes were tunable by altering the polymerization time. Composition of the polymer layer could be tuned by the monomers, for example, polystyrene (PS) layer was achieved by ATRP of styrene. Sulfonated PS layer (sPS) can be derived by the sulfonation of the PS layer. By specific interactions of desired materials with the sPS gel, a favorable growth of other materials, for example, metallic Ni, conductive polyaniline, inorganic titania is allowed. Besides, sPS can self-catalyze into carbon at high temperature. Thus, the composition of the composite layers can be broadly controlled ranging within metal or metallic compounds, polymer, inorganic, carbon, and their composites. This concept is general and can be extended to other polymeric gels and grown materials, expecting a huge family of composite nanotube. © 2009 Wiley Periodicals, Inc. J Appl Polym Sci 112: 2647–2655, 2009

Key words: haglloysite; nanotube; ATRP; polymeric gel; composite

INTRODUCTION

Nanotubes with a hollow cavity have attracted a great deal of interest in both scientific and industrial fields. They possess novel physical and chemical properties derived from the structural versatility and provide opportunities for advanced applications in the fields of electronics, optics, catalysis, energy storage, and biological systems.[1–5] Various types of nanotubes have been synthesized, such as carbon,[6] metallic,[7–12] inorganic,[13–19] and polymeric[20,21] nanotubes by different methods including hydrothermal synthesis, surfactant-assisted synthesis, and decomposition. One of the extensively used methods for producing nanotubes is template synthesis within porous membranes.[22,23] During the template synthesis, a variety of strategies are used[24] such as electrochemical deposition, electroless deposition, layer-by-layer assembly, wetting approach, polymerization, sol–gel deposition, and chemical vapor deposition. Although nanotubes can be prepared with well-controlled structures, strict conditions are required and the porous membrane templates should be sacrificed. Besides, the synthesis procedure cannot be scaled up for massive production. It is required to develop a general and facile method to massively synthesize nanotubes with varied composition.

Recently, halloysite as an economically available nanotubular raw material has gained growing interest in the synthesis of complex structures.[25–28] Halloysite is mainly composed of a two-layered aluminosilicate (composition: $Al_2Si_2O_5(OH)_4H_2O$), chemically similar to kaolin, which has a predominantly hollow tubular structure in the submicrometer range.[25–28] Electroless and layer-by-layer-assisted deposition are mainly used to fabricate halloysite-based composites.[29,30] However, the former method is restricted to metallic/halloysite composites, whereas the latter is limited to those species with strong driving force such as electrostatic interactions.

It will be promising to develop a new template synthesis of composite nanotubes with varied composition. As well known, the physical and chemical environment of polymeric gels can be greatly tuned, and they can be used as templates to induce a favorable growth of materials with varied composition through specific interactions.[31–39] We have recently reported the synthesis of polymer/halloysite composite via a surface-initiated atom transfer radical

Correspondence to: Z. Yang (yangzz@iccas.ac.cn).
Contract grant sponsor: NSFC; contract grant numbers: 50573083, 50733004, 20720102041.
Contract grant sponsor: China Ministry of Science and Technology; contract grant number: 2006CB605300.

polymerization (ATRP) onto the halloysite nanotube,[40] and the composition and thickness of the polymeric layer could be easily tuned by either alteration the monomer feeding or the reaction time. We have previously reported derivation of sulfonated polystyrene gels with tunable proton ion content by the sulfonation of polystyrene colloids and their template synthesis of other materials.[34–39] By further extending our method to halloysite/polymer composite nanotubes, it is expected to synthesize halloysite composite nanotubes. Bearing in mind the capability of forming specific interactions of sulfonic acid group (—SO_3H) with other materials, we expect to develop a general and scalable method to prepare composite halloysite.

As previously reported, PS/halloysite composite nanotubes have been prepared using the surface-initiated ATRP. After the introduction of sulfonic acid group (—SO_3H) by sulfonation, desired materials can be favorably grown within the sulfonated PS layer by specific interactions resulting in composite layer, whose composition can be varied within polymers, inorganic materials, metals, and their compounds. Furthermore, the sulfonic acid group can self-catalyze the carbonization, deriving halloysite-carbon-based composite nanotubes.

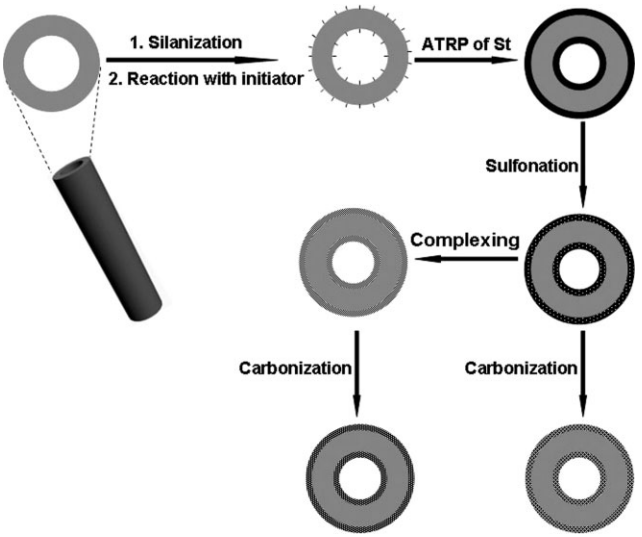

Scheme 1 Illustrative synthesis of halloysite-based composite nanotubes. Gray area represents halloysite nanotube; short line represents the ATRP initiator group; black solid area represents PS layer; black dot area represents sPS layer; and black grid area represents composite layer.

EXPERIMENTAL

Immobilization of ATRP initiator onto halloysite nanotubes

The halloysite nanotubes were immobilized with an ATRP initiator by a two-step method.[40] After being treated with H_2O_2 at 80°C for 24 h, the halloysite was modified with 3-aminopropyltrimethoxysilane (APS) at 120°C in toluene for 12 h and then washed with ethanol. The silanized halloysite was further reacted with 2-bromoisobutyryl bromide in dry dichloromethane containing dry triethylamine at 25°C for 10 h. After the modified halloysite was repeatedly washed with acetone and ethanol, it was dried under vacuum before use.

Synthesis of crosslinked PS/halloysite composite nanotubes

In a typical experiment, 0.8 g (0.046 mmol initiator) of modified halloysite, 10 mL (87.4 mmol) of styrene (St), 2.3 g (17.7 mmol) of divinylbenzene (DVB), 10 mL of toluene, and 144 μL (0.7 mmol) of *N*,*N*,*N*′,*N*″,*N*″-pentamethyldiethylenetriamine (PMDETA) were mixed in a 50-mL dry flask equipped with a magnetic stirrer. After being purged with nitrogen, 0.03 g (0.2 mmol) of CuBr was added. Afterward, ATRP was carried out at 110°C for a varied time to control the grafting polymer content. Three representative crosslinked PS/halloysite composite nanotubes PS_1/halloysite, PS_2/halloysite, and PS_3/halloysite were achieved by polymerization for 1, 2, and 3 h, respectively.

Sulfonation of the crosslinked PS/halloysite composites

The freezed-dried crosslinked PS/halloysite powders were immersed in excess concentrated sulfuric acid at 40°C for 24 h to derive a sulfonated polystyrene gel layer.[34] The sulfonated PS/halloysite composites were denoted as sPS/halloysite. For example, sPS_1/halloysite represents the sulfonated PS/halloysite nanotube derived from the composite nanotube synthesized by ATRP for 1 h.

Ni/carbon/halloysite composite nanotubes

In a typical experiment, 0.05 g dried sPS/halloysite was dispersed in 10 mL of 0.2*M* nickel nitrate aqueous solution. After 12 h, nickel nitrate-saturated sPS/halloysite was separated by centrifugation and further washed with water to remove residual salt outside the composite. Then, the freeze-dried composites were heated in a glass tube with alcohol burner, the atmosphere was H_2 leading to Ni/carbon/halloysite composite nanotubes.

Conductive polyaniline (PANi)/sPS/halloysite composite nanotubes

Dried sPS/halloysite (0.05 g) was dispersed in 10 mL of water, and then a desired amount of aniline monomer was added into the aqueous dispersion

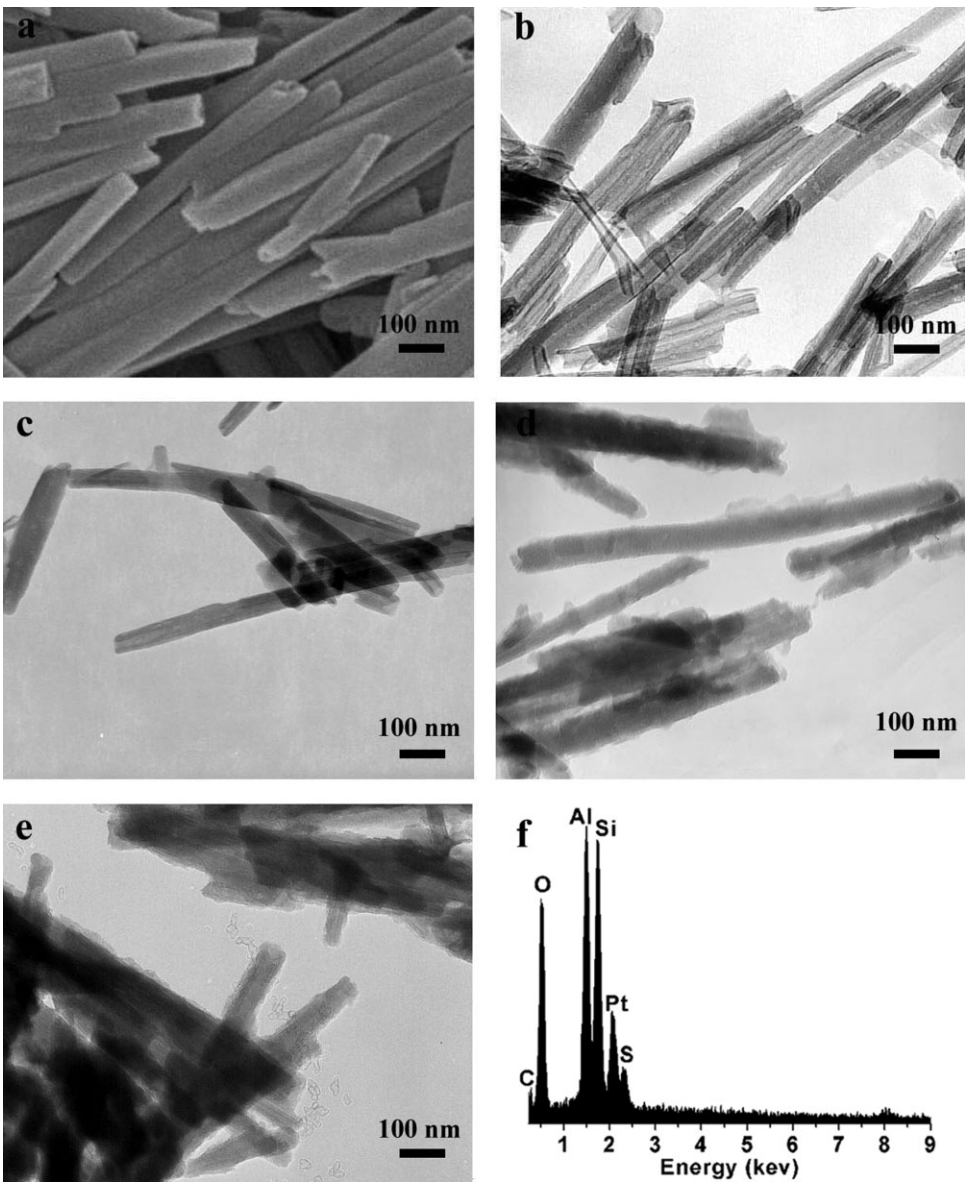

Figure 1 (a and b) Representative SEM and TEM images of the halloysite nanotube; (c and d) TEM images of the PS/halloysite composite nanotubes obtained via ATRP at 110°C for polymerization 2 and 3 h, respectively; (e) TEM image of the sPS_2/halloysite composite nanotube derived from the sample as shown in (c); f) corresponding EDX spectrum of the sample as shown in (e), revealing the presence of S (Pt peak from the sputtered Pt).

under stirring for 24 h to allow a complete adsorption. A desired amount of aqueous initiator ammonium persulfate (2*M*) was added to allow a polymerization of aniline at room temperature for 12 h. The PANi/sPS/halloysite composite nanotubes were purified by centrifugation and washed with water.

Titania/sPS/halloysite composite nanotube

Dried sPS/halloysite (0.05 g) was dispersed in 2 mL of tetrabutyl titanate (TBT) under stirring for 24 h. After the TBT saturated sPS/halloysite was separated by centrifugation and washed with ethanol to remove residual TBT outside the nanotube, they were redispersed in 4 mL of ethanol. Water (4 mL) was dropped into the dispersion under stirring followed by a sol–gel process for 6 h at ambient temperature. The composite nanotubes were centrifugated and washed with ethanol/water.

Carbonization

After the crosslinked PS/halloysite composite powder was preoxidated at 200°C for 2 h in an air atmosphere, it was further heated to 370°C at 2°C/min. After being held at 370°C for 4 h, the temperature was further increased to 800°C and held for 2 h

in nitrogen to prepare carbon composites. Free carbon nanocomposites were formed by dissolution of the halloysite with a HF/HCl mixture (the volume ratio is 1 : 1).

Characterization

Morphology and composition of the samples were performed with a Hitachi S-4300 scanning electron microscope (SEM) equipped with an energy-dispersive X-ray (EDX) analyzer operating at an accelerating voltage of 15 kV. The samples were dispersed in ethanol under ultrasonication and dropped onto carbon-coated copper grids for transmission electron microscopy (TEM) characterization (JEOL 100CX operating at 100 kV). Elemental analysis was carried out using a Flash EA-1112 apparatus. The dried samples were pressed into pellets with potassium bromide (KBr) and characterized by a BRUKER EQUINOX 55 FTIR spectrophotometer. The crystalline phases of the materials were characterized by wide-angle X-ray powder scattering (Rigaku D/max-2500).

RESULTS AND DISCUSSION

As illustrated in Scheme 1, a commercial halloysite nanotube was selected as an example parent template.[41] After being modified with silanes and 2-bromoisobutyryl bromide, ATRP of styrene was carried out synchronously onto both the interior and exterior wall surfaces to gain PS/halloysite nanotubes. After conversion of PS into sulfonated PS by sulfonation introducing sulfonic acid group (—SO_3H), a diversity of desired materials could be favorably grown within the sPS layer by specific interactions. After being carbonized at high temperature, carbon-based composite layer was derived.

The halloysite is predominately tubular with a length of 1–2 μm and an inner diameter of 20–30 nm. The shell thickness is 10–15 nm [Fig. 1(a,b)]. After being modified with APS and 2-bromoisobutyrate, FTIR spectra of the modified halloysite (ha-Br) (trace b, Fig. 2) showed sharp vibration bands at 3000–2870 and 1540 cm^{-1} diagnostic for the saturated hydrocarbon and amide II (—CONH—), which were not present in the IR spectra of the starting halloysite (trace a, Fig. 2), indicating that the ATRP initiator was successfully incorporated onto the halloysite. Further elemental analysis showed an average immobilization amount of the initiator of 0.058 mmol/g halloysite. The surface-modified halloysite nanotubes were then grafted by ATRP of styrene at 110°C. The PS thickness of both the exterior and interior layers could be tuned by polymerization time [Fig. 1(c,d)].[40] Herein, we focused on the PS/halloysite composite nanotubes whose interior cavity was not completely filled with polymer layer. For example, after being polymerized for 2 h, the average interior cavity diameter decreased to several nanometers [Fig. 1(c)]. The characteristic bands between 2950 and 2850 cm^{-1} were assigned to the hydrocarbon backbone of PS (trace c, Fig. 2), which strengthened when compared with the FTIR spectra of the modified halloysite (ha-Br) (trace b, Fig. 2).

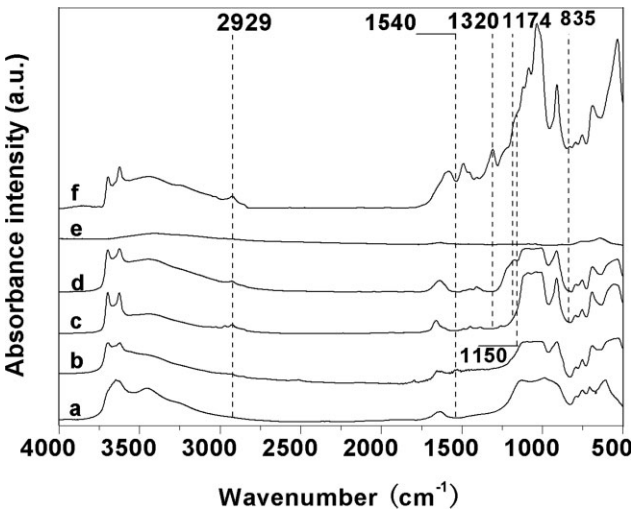

Figure 2 FTIR spectra of some representative halloysite nanocomposites: (a) the halloysite; (b) the modified halloysite with the initiator; (c) the PS/halloysite composite; (d) sPS/halloysite composite; (e) carbon composite after halloysite was dissolved from the C/halloysite composite; (f) PANi/sPS/halloysite composite. The characteristic band at 1540 cm^{-1} was assigned to amide II (—CONH—), which appeared after the ATRP initiator was immobilized. The characteristic bands at 1174 cm^{-1} were assigned to the derived sulfonic acid group (—SO_3H). The bands at 1320 (C—N stretch), 1150 (C—H plane bend), and 835 cm^{-1} (1, 4-disubstituted benzene ring stretch) were identical to the emeraldine salt form PANi. The characteristic bands between 2950 and 2850 cm^{-1} were assigned to the hydrocarbon $\text{—}(CH_2\text{—}\underset{|}{CH})_n\text{—}$ backbone.

To demonstrate the conversion of PS layer into functional layer such as sulfonated PS layer, the PS/halloysite nanotubes were treated with concentrated sulfuric acid at 40°C for 24 h to derive a completely sPS gel layer [Fig. 1(e)]. The sulfonic acid group (—SO_3H) was verified by FTIR spectra (trace d, Fig. 2). The characteristic band at 1174 cm^{-1} attributed to the derived sulfonic acid group (—SO_3H).[34–39] The tubular structure was well preserved after sulfonation [Fig. 1(e)]. Sulfur element was detected by EDX [Fig. 1(f)], further indicating the presence of sulfonic acid group (—SO_3H).

Since the sulfonic acid group can easily complex with metal ions, many metal nanoparticles were thus prepared by reduction within the layer. As an example, after the sPS/halloysite composite nanotubes were immersed in nickel nitrate aqueous

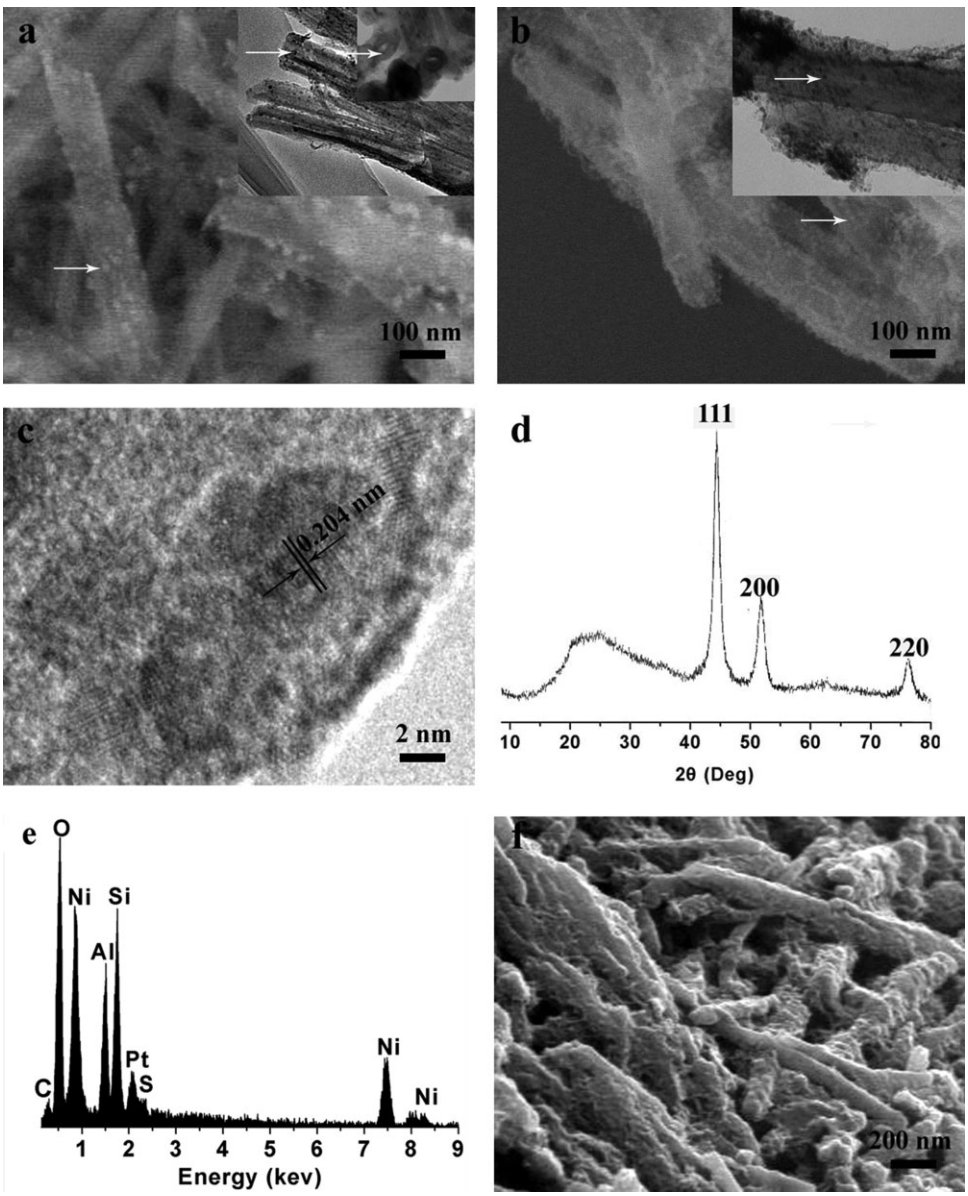

Figure 3 (a and b) Representative SEM and TEM images of Ni/C/halloysite composite derived from sPS_1/halloysite nanotubes and sPS_2/halloysite nanotubes, respectively; (c and d) corresponding HRTEM image and X-ray powder diffraction spectrum of the sample as shown in (a), revealing the face-centered cubic (fcc) nickel structure; (e) corresponding EDX spectrum of the sample as shown in (b), revealing the existence of Ni (Pt peak from the sputtered Pt); (f) SEM image of Ni/C/halloysite nonwoven fabric.

solution and further reduced in an H_2 atmosphere at high temperature, Ni/C/halloysite composite was derived (note: owing to the catalytic carbonization by the sulfonic acid group,[42] the sPS layers were easily converted into carbon at high temperature). Ni nanoparticles with a mean size of about 10 nm were formed within the carbon layer, which were well distributed through the whole carbon layer [Fig. 3(a,b)]. The top right corner of Figure 3(a) was the cross-section image of Ni/C/halloysite, Ni particle can be observed in the cavity (marked with the arrow), indicating the interior of the tube was coated with Ni. The amount of Ni nanoparticles and the morphology could be tuned. Within the sPS_1/halloysite nanotubes derived from those PS/halloysite nanotubes by polymerization for 1 h, Ni nanoparticles were sparsely distributed within the carbon layer [Fig. 3(a)]. With prolonged polymerization time, the Ni nanoparticles aggregated, so the dimension seems in excess 100 nm in some area. Eventually, a layer composed of Ni nanoparticles was formed [Fig. 3(b)]. This was consistent with increasing sulfonic acid group content, indicated by the element S [1.01 wt % (sPS_1/halloysite), 1.92 wt % (sPS_2/halloysite)]. The crystallinity of the nanoparticles and nanotubes was characterized using XRD

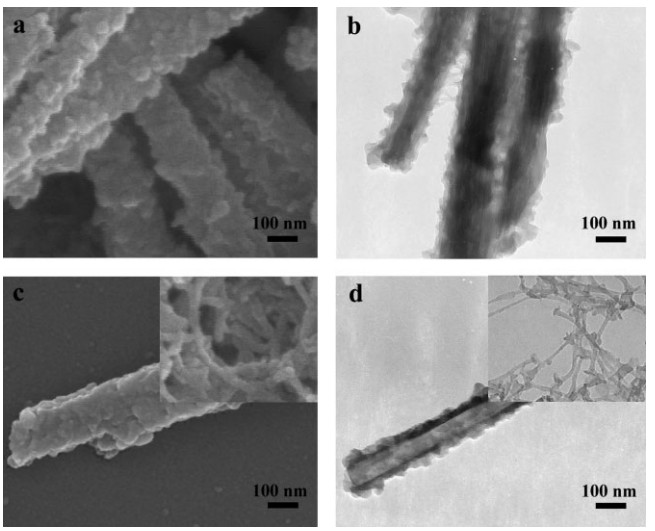

Figure 4 SEM and TEM images of some representative conductive PANi/sPS/halloysite composite: (a and b) PANi/sPS_2/halloysite composite; (c and d) PANi/sPS_2 composite nanotube and nanowire after the halloysite was dissolved by HF/HCl mixture with the volume ratio of 1 : 1.

[Fig. 3(d)], consistent with JCPDS standard card 04-0850. The peaks at $2\theta = 44.40°$, 51.72°, 76.20° were assigned as the (111), (200), (220) reflection lines. The Ni nanoparticles were calculated to be about 10 nm from the XRD, consistent with the TEM result [Fig. 3(a)]. The face-centered cubic (fcc) nickel structure was further verified by HRTEM [Fig. 3(c)]. EDX analysis demonstrated that the Ni content of the samples Ni/$carbon_1$/halloysite and Ni/$carbon_2$/halloysite were 9.23 wt % and 25.2 wt %, respectively [Fig. 3(e)]. The method can be extended to grow other magnetic materials (Co, Fe_3O_4) and metal nanoparticles (Ag, Au, Pt, and Pd) within the sPS layer, achieving the corresponding composite nanotubes.[34–39] Composition control of nanotubes will be promising for the separation of biomolecules, MRI contrast agent, hyperthermia, biosensor, and target drug delivery.[43–45] Besides individual Ni/carbon/halloysite composite nanotubes, the corresponding nonwoven fabrics could be easily prepared by casting dispersion of the individual sPS/halloysite composite nanotubes, followed by the similar procedure of preparation of Ni/carbon/halloysite composite nanotubes [Fig. 3(f)].

Besides metallic composite nanotubes, the method can be extended to functional polymers. Conductive polyaniline (PANi) composite nanotubes were prepared to demonstrate this concept. Monomer aniline was favorably adsorbed within the sPS layer by specific interaction and polymerized forming PANi/sPS/halloysite composite. The sPS_2/halloysite nanotubes derived from those PS/halloysite nanotubes by a polymerization for 2 h was used to complex with PANi [Fig. 4(a,b)]. The whole composite became dark green after being complexed with PANi. PANi was *in situ* doped by sPS in the form of emeraldine salt evidenced by FTIR spectra (trace f, Fig. 2). The bands at 1320 (C—N stretch), 1150 (C—H plane bend), and 835 cm^{-1} (1,4-disubstituted benzene ring stretch) were identical to the emeraldine salt form PANi.[46] Comparing with the parent sPS_2/halloysite composite nanotubes [Fig. 1(e)], diameter of the conductive composite nanotube increased dramatically from 40–60 nm to 100–120 nm, and the cavity was completely filled [Fig. 4(a,b)], implying both the exterior and interior of the tubes were coated with PANi. The gray region of the TEM image was attributed to the PANi/sPS composite layer [Fig. 4(b)]. After the halloysite was dissolved with HF/HCl mixture (the volume ratio was 1 : 1), the PANi/sPS_2 composite nanotubes and composite nanowires were derived with the structure well preserved [Fig. 4(c,d)].

The sulfonic acid group (—SO_3H) could also catalyze the sol–gel process of TBT forming titania therein [Fig. 5(a,b)]. The surface became coarse with titania as confirmed by SEM and EDX analysis [Fig. 5(f)]. It is worth to note that owing to the catalytic carbonization by the sulfonic acid group,[42] the sPS layers were easily converted into carbon at high temperature. The titania/carbon/halloysite composite nanotubes were formed after being treated at high temperature in nitrogen, which will be discussed later. After being calcined at 450°C in nitrogen, the phase transformed from amorphous to anatase (trace b, Fig. 6). At a high temperature, for example 600°C, anatase-titania/carbon/halloysite composite nanotubes were derived (trace c, Fig. 6). At 900°C, pure rutile phase was achieved but the composite nanotubes were coalesced (trace d, Fig. 6). To show the distribution of titania within the sPS layer, the titania/sPS/halloysite composite nanotube was calcined at 600°C in air to remove the polymer. The TEM image showed that the composite layer became less dense with the tubular structure well preserved, confirming that the titania formed a continuous network within the sPS matrix. EDX analysis showed that the Ti content of the samples titania/sPS_1/halloysite and titania/sPS_2/halloysite were 9.9 and 21.5 wt %, respectively.

Carbonization process can be catalyzed by the sulfonic acid (—SO_3H) to convert the polymer into carbon.[42] Along the similar process, sPS/halloysite composite nanotube was converted into a carbon/halloysite composite at 800°C [Fig. 7(a,b)]. The formation of carbon was verified by FTIR spectra (trace e, Fig. 2). Raman spectrum [two bands at 1590 and 1320 cm^{-1} corresponding to G and D bands, Fig. 8(a)][42] and XRD [Fig. 8(b)] indicated that the formed carbon was amorphous. A thicker sPS layer of sPS_2/halloysite could more easily result carbon

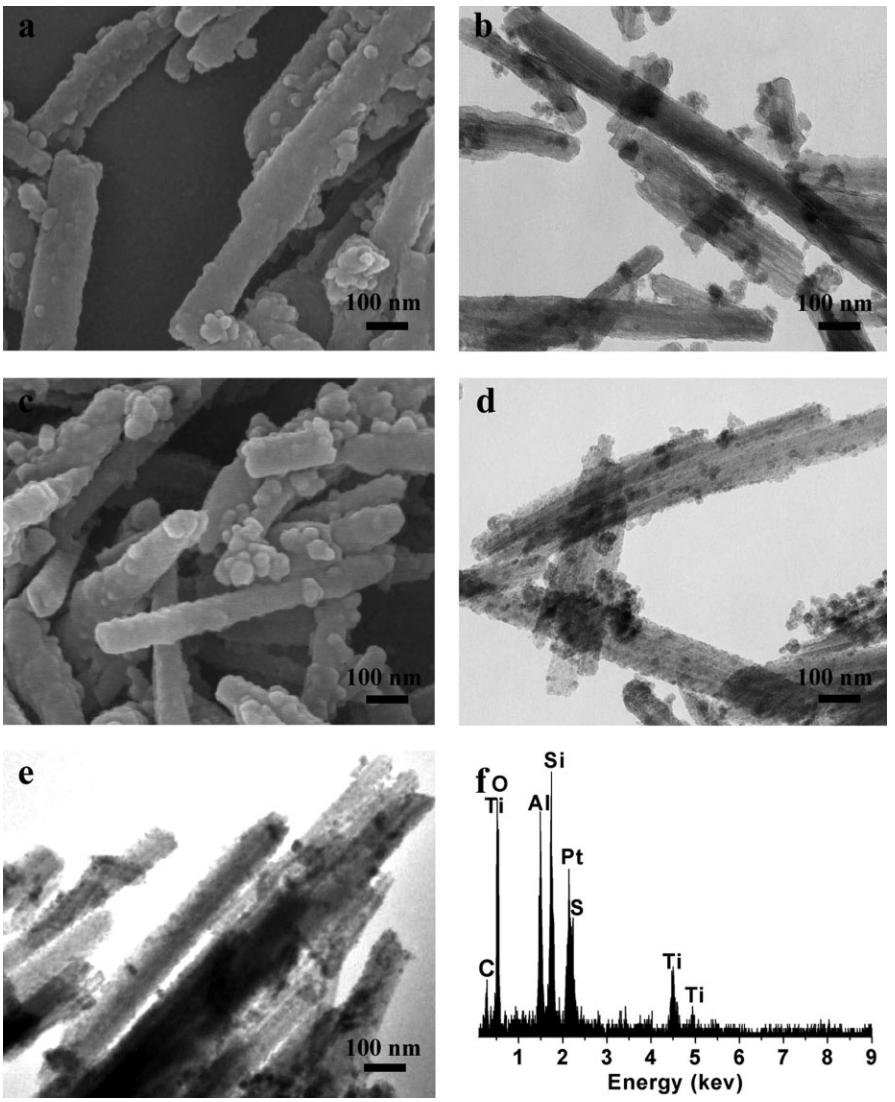

Figure 5 SEM and TEM images of some representative titania/sPS/halloysite composite nanotubes: (a and b) titania/sPS/halloysite composite nanotube before being calcined; (c and d) titania/C/halloysite composite nanotube after being calcined at 600°C for 2 h in nitrogen; (e) titania/halloysite composite nanotube after being calcined at 600°C for 2 h in air; (f) corresponding EDX spectrum of the sample as shown in (a), revealing the presence of TiO_2 (Pt peak from the sputtered Pt).

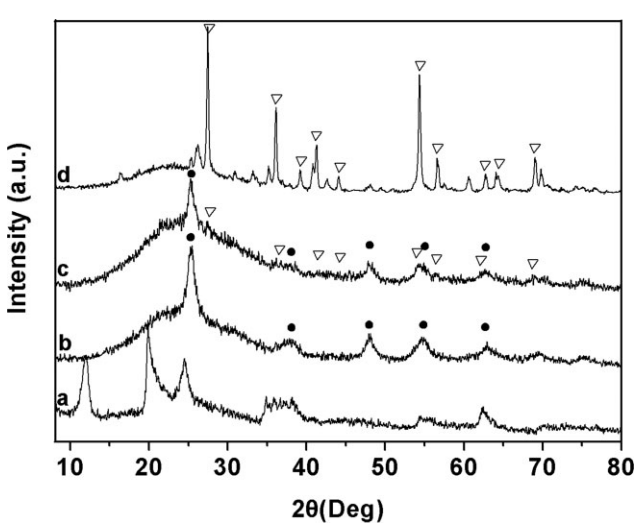

Figure 6 XRD spectra of (a) titania/sPS/halloysite composite nanotube untreated; (b–d) titania/C/halloysite composite nanotube after being calcined at 450, 600, and 900°C for 2 h in nitrogen, respectively. ▽ = rutile (JCPDS No. 21-1276); ● = anatase (JCPDS No. 21-1272).

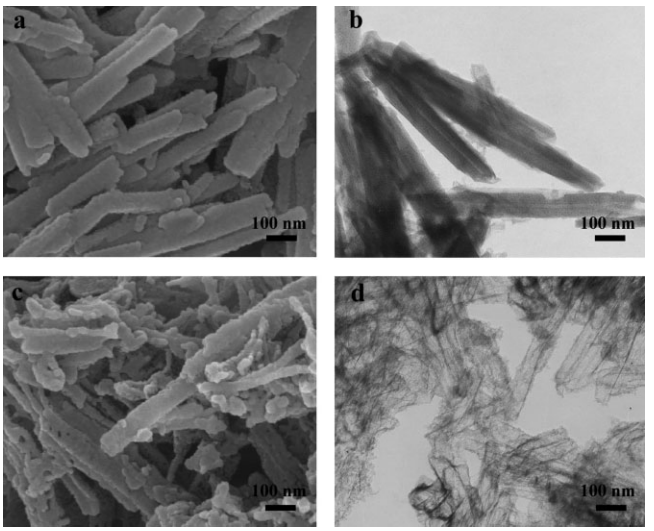

Figure 7 SEM and TEM images of some representative carbon samples: (a and b) the C/halloysite composite nanotubes after the sPS/halloysite composite was carbonized at 800°C; (c and d) C composites after the halloysite was dissolved from the C/halloysite composite.

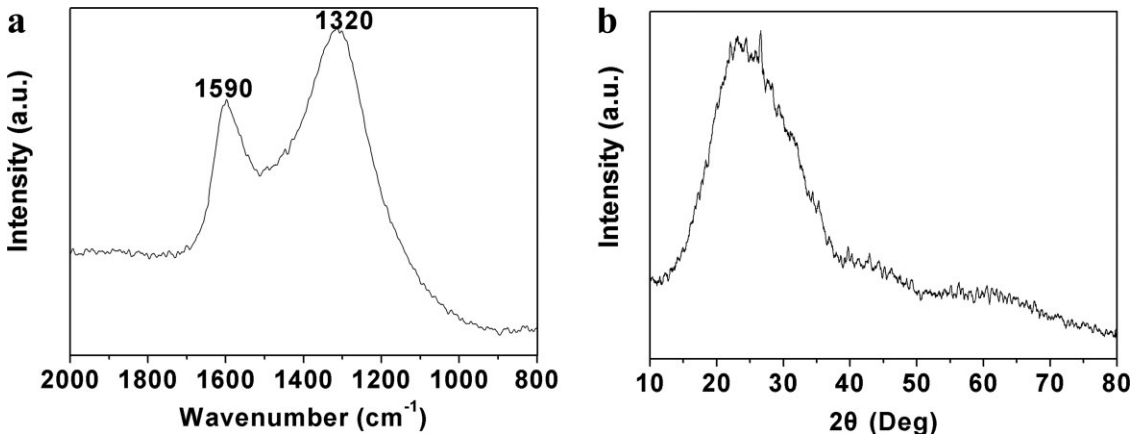

Figure 8 (a) Raman spectrum and (b) XRD spectra of the carbon composite after the halloysite was dissolved from the C/halloysite composite.

nanocomposites after the halloysite was dissolved [Fig. 7(c,d)]. The aforementioned procedures can be combined, deriving carbon-based composite nanotubes, for example, the Ni/carbon/halloysite and titania/carbon/halloysite.

CONCLUSIONS

We have demonstrated a general template synthesis halloysite-based composite nanotubes. Starting from a parent halloysite nanotube, polymer composite nanotubes were synthesized by ATRP. The shell thickness and the cavity size of the polymer composite nanotubes were tunable by altering the polymerization time. Composition of the polymer layer could be tuned by the monomers, for example, PS layer was achieved by ATRP of styrene. Sulfonated polystyrene layer can be derived by sulfonation of the PS layer, further tuning physicochemical environment of the polymer layer. By specific interactions of desired materials with the sPS gel, a favorable growth of other materials is allowed. Besides, sPS can self-catalyze into carbon at high temperature. Composition of the composite layers can be broadly controlled ranging within metal or metallic compounds, polymer, inorganic, carbon, and their composites. This concept is general and can be extended to other polymeric gels and grown materials, expecting a huge family of composite nanotubes.

References

1. Xia, Y.; Yang, P.; Sun, Y.; Wu, Y.; Mayers, B.; Gates, B.; Yin, Y.; Kim, F.; Yan, H. Adv Mater 2003, 15, 353.
2. Patzke, G. R.; Krumeich, F.; Nesper, R. Angew Chem Int Ed 2002, 41, 2446.
3. Zhang, X.; Manohar, S. K. J Am Chem Soc 2004, 126, 12714.
4. Huang, J.; Virji, S.; Weiller, B. H.; Kaner, R. B. J Am Chem Soc 2003, 125, 314.
5. Hughes, M.; Chen, G. Z.; Shaffer, M. S. P.; Fray, D. J.; Windle, A. H. Chem Mater 2002, 14, 1610.
6. Iijima, S. Nature 1991, 354, 56.
7. Carny, O.; Shalev, D. E.; Gazit, E. Nano Lett 2006, 6, 1894.
8. Sun, Y.; Xia, Y. Adv Mater 2004, 16, 264.
9. Sehayek, T.; Lahav, M.; Popovitz-Biro, R.; Vaskevich, A..; Rubinstein, I. Chem Mater 2005, 17, 3743.
10. Steinhart, M.; Jia, Z. H.; Schaper, A. K.; Wehrspohn, R. B.; Gosele, U.; Wendorff, J. H. Adv Mater 2003, 15, 706.
11. Kijima, T.; Yoshimura, T.; Uota, M.; Ikeda, T.; Fujikawa, D.; Mouri, S.; Uoyama, S. Angew Chem Int Ed 2004, 43, 228.
12. Chen, J.; Tao, Z. L.; Li, S. L. J Am Chem Soc 2004, 126, 3060.
13. Hwang, J.; Min, B. J.; Lee, S.; Keem, K.; Cho, K.; Sung, M. Y.; Lee, M. S.; Kim, S. Adv Mater 2004, 16, 422.
14. Zhang, H.; Quan, X.; Chen, S.; Zhao, H. Environ Sci Technol 2006, 40, 6104.
15. Li, D.; Xia, Y. Nano Lett 2004, 4, 933.
16. Li, Y. D.; Li, X. L.; He, R. R.; Zhu, J.; Deng, Z. X. J Am Chem Soc 2002, 124, 1411.
17. Kong, X. Y.; Ding, Y.; Wang, Z. L. J Phys Chem B 2004, 108, 570.
18. Bao, J.; Xu, D.; Zhou, Q.; Xu, Z.; Feng, Y.; Zhou, Y. Chem Mater 2002, 14, 4709.
19. Wu, G.; Zhang, L.; Cheng, B.; Xie, T.; Yuan, X. J Am Chem Soc 2004, 126, 5976.
20. Mayya, K. S.; Gittins, D. I.; Dibaj, A. M.; Caruso, F. Nano Lett 2001, 1, 727.
21. Jang, J.; Yoon, H. Langmuir 2005, 21, 11484.
22. Martin, C. R. In Electroanalytical Chemistry; Bard, A. J.; Rubinstein, I., Eds. Marcel Dekker: New York, 1999; Vol. 21.
23. Hulteen, J. C.; Martin, C. R. J Mater Chem 1997, 7, 1075.
24. Caruso, R. A.; Schattka, J. H.; Greiner, A. Adv Mater 2001, 13, 1577.
25. Joussein, E.; Petit, S.; Churchman, J.; Theng, B.; Righi, D.; Delvaux, B. Clay Miner 2005, 40, 383.
26. Antill, S. J. Aust J Chem 2003, 56, 723.
27. Shchukin, D. G.; Sukhorukov, G. B.; Price, R. R.; Lvov, Y. M. Small 2005, 1, 510.
28. Lu, Z.; Eadula, S.; Zheng, Z.; Xu, K.; Grozdits, G.; Lvov, Y. Colloids Surf A 2007, 292, 56.
29. Fu, Y.; Zhang, L. J Solid State Chem 2005, 178, 3595.
30. Shchukin, D. G.; Lamaka, S. V.; Yasakau, K. A.; Zheludkevich, M. L.; Ferreira, M. G. S.; Mohwald. H. J Phys Chem C 2008, 112, 958.
31. Caruso, R. A.; Antonietti, M.; Giersig, M.; Hentze, H. P.; Jia, J. Chem Mater 2001, 13, 1114.
32. Ziolo, R. F.; Giannelis, E. P.; Weinstein, B. A.; O'Horo, M. P.; Ganguly, B. N.; Mehrotra, V.; Russell, M. W.; Huffman, D. R. Science 1992, 257, 219.
33. Breulmann, M.; Davis, S. A.; Mann, S.; Hentze, H. P.; Antonietti, M. Adv Mater 2000, 12, 502.

34. Yang, Z. Z.; Niu, Z. W.; Lu, Y. F.; Hu, Z. B.; Han, C. C. Angew Chem Int Ed 2003, 42, 1943.
35. Niu, Z. W.; Yang, Z. Z.; Hu, Z. B.; Lu, Y. F.; Han, C. C. Adv Funct Mater 2003, 13, 949.
36. Yang, Z. Z.; Li, D.; Rong, J. H.; Yan, W. D.; Niu, Z. W. Macromol Mater Eng 2002, 287, 627.
37. Rong, J. H.; Ma, J.; Yang, Z. Z. Macromol Rapid Commun 2004, 25, 1786.
38. Yang, M.; Ma, J.; Niu, Z. W.; Xu, H. F.; Meng, Z. K.; Lu, Y. F.; Yang, Z. Z. Adv Funct Mater 2005, 15, 1523.
39. Yang, M.; Ma, J.; Zhang, C. L.; Lu, Y. F.; Yang, Z. Z. Angew Chem Int Ed 2005, 44, 6727.
40. Li, C. P.; Liu, J. G.; Qu, X. Z.; Guo, B. C.; Yang, Z. Z. J Appl Polym Sci 2008, 110, 3638.
41. Technical Report of Imerys Tableware Asia Limited. Available at: http://www.imerys-tableware.com/halloy.html.
42. Ding, S. J.; Zhang, C. L.; Qu, X. Z.; Liu, J. G.; Lu, Y. F.; Yang, Z. Z. Colloid Polym Sci 2008, 286, 1093.
43. Safarik, I.; Safarikova, M. J Chromatogr B 1999, 722, 33.
44. Halavaara, J.; Tervahartiala, R.; Isoniemi, H.; Hockerstedt, K. Acta Radiol 2002, 43, 180.
45. Lubbe, A. S.; Alexiou, C.; Bergemann, C. J Surg Res 2001, 95, 200.
46. Wei, Z. X.; Wan, M. X. Adv Mater 2002, 14, 1314.